# CONGA-PIC : COnforming/Non-conforming GAlerkin solvers coupled with Particle-In-Cell schemes

Martin Campos-Pinto, Frédérique Charles, Mathieu Lutz, Marie Mounier

CIRM, Luminy, July 28 - August 29 2014

# Outline

# Introduction

# Introduction : Transverse Electric Maxwell-Vlasov system

Transverse Electric (TE) Maxwell system in 2d

$$\begin{cases} \partial_t E - c^2 \,\mathbf{curl}\, B = -\frac{1}{\varepsilon_0} J, \\ \partial_t B + \mathrm{curl}\, E = 0, \\ \mathrm{div}\,(E) = \dfrac{\rho}{\varepsilon_0}, \end{cases}$$

where the source terms

$$\begin{cases} \rho(t,x) := q \displaystyle\int_{\mathbb{R}^2} f(t,x,v)\,\mathrm{d}v, \\ J(t,x) := q \displaystyle\int_{\mathbb{R}^2} v f(t,x,v)\,\mathrm{d}v. \end{cases}$$

are derived from the four dimensional Vlasov equation

$$\partial_t f + v \cdot \nabla_x f + \frac{q}{m}(E + v^\perp B) \cdot \nabla_v f = 0,$$

# Introduction : The divergence equation

Taking formally the divergence of the Ampere equation we obtain

$$\partial_t \mathrm{div}\,(E) = -\frac{1}{\epsilon_0}\mathrm{div}\,(J).$$

Thus, if the Gauss equation is satisfied at $t = 0$ :

$$\underbrace{\mathrm{div}\,(\mathbf{E}) = \rho/\varepsilon_0}_{\text{Gauss law}} \quad \Leftrightarrow \quad \underbrace{\partial_t \rho + \mathrm{div}\,(\mathbf{J}) = 0}_{\text{Continuity equation}} \quad \longleftarrow \text{Intrinsic property of Vlasov.}$$

**Numerical level :**

- ⋆ Numerical schemes need to satisfy discrete analogs of the Gauss law and of the continuity equation.
- ⟶ Discrete analog of the Gauss law concerns the consistency of the Maxwell solver (that involve only the curl equations).
- ⟶ Discrete analog of the continuity equation concerns the consistency of the Vlasov solver (specially the way to compute the current).

# Introduction : Outline of the numerical method

**The Maxwell Solvers :** We will compare two Galerkin solvers :

- A conforming solver (FEM based on conforming discrete spaces of functions).
- A conforming / non-conforming solver (Conga).

$\longrightarrow$ They satisfy a discrete analog of the Gauss equation.

$\longrightarrow$ They preserve a strong Ampere equation at the discrete level.

$\longrightarrow$ As DG, Conga does not require to invert a global mass matrix.

**Vlasov Solver :** Particle-In-Cell method.

**Test cases :** Weibel instability, diode, magnetron :

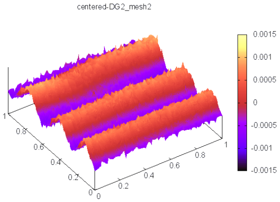


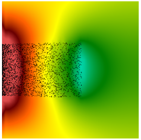

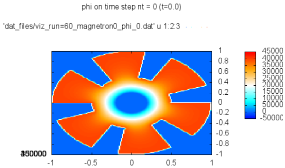

# The Maxwell Solvers

# Galerkin Solver for Maxwell

- Test cases (Weibel, diode, magnetron) involve Silver-Müller boundary condition

$$E \times n = \begin{cases} 0 & \text{on } \Gamma_M \\ c(B \times n) \times n = -cB & \text{on } \Gamma_A. \end{cases}$$

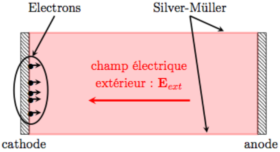


$\Gamma_A$ : Artificial boundary used to limit the computational domain.

- Integrating by parts the curl term in the Faraday equation

$$\begin{cases} \langle \partial_t E, \varphi^\varepsilon \rangle - c^2 \langle \mathbf{curl}\, B, \varphi^\varepsilon \rangle = -\dfrac{1}{\varepsilon_0} \langle J, \varphi^\varepsilon \rangle, & \forall \varphi^\varepsilon \in V^\varepsilon = H(\mathrm{div}; \Omega) \\ \langle \partial_t B, \varphi^\mu \rangle + \langle E, \mathbf{curl}\, \varphi^\mu \rangle + c \langle B, \varphi^\mu \rangle_{\Gamma_A} = 0, & \forall \varphi^\mu \in V^\mu = H(\mathbf{curl}; \Omega). \end{cases}$$

From this weak formulation we will deduce two semi-discrete schemes.

# Galerkin Solver – The conforming scheme

Find $(E_h, B_h) \in \mathcal{C}^1([0,T]; V_h^\varepsilon \times V_h^\mu)$ solution to

$$\begin{cases} \langle \partial_t E_h, \boldsymbol{\varphi}^\varepsilon \rangle - c^2 \langle \mathbf{curl}\, B_h, \boldsymbol{\varphi}^\varepsilon \rangle = -\frac{1}{\varepsilon_0} \langle \pi_h^{\mathrm{div}} J, \boldsymbol{\varphi}^\varepsilon \rangle, & \boldsymbol{\varphi}^\varepsilon \in V_h^\varepsilon \subset H(\mathrm{div}\,;\Omega) \\ \langle \partial_t B_h, \varphi^\mu \rangle + \langle E_h, \mathbf{curl}\, \varphi^\mu \rangle + c \langle B_h, \varphi^\mu \rangle_{\Gamma_A} = 0, & \varphi^\mu \in V_h^\mu \subset H(\mathbf{curl};\Omega) \end{cases}$$

In the code we shall use :

$$V_h^\mu = \mathcal{L}_p(\Omega, \mathcal{T}_h) \xrightarrow{\mathbf{curl}} V_h^\varepsilon = \mathcal{RT}_{p-1}(\Omega, \mathcal{T}_h) \xrightarrow{\mathbf{div}} V_h^2 = \mathcal{P}_{p-1}(\mathcal{T}_h)$$

and $\pi_h^{\mathrm{div}}$ is the Raviart-Thomas finite element interpolation.

- ⋆ Traditional FEM use an orthogonal projector $P_h$ instead of $\pi_h^{\mathrm{div}}$.
  $\longrightarrow$ The degrees of freedom are integrals on triangles and edges (local).
- ⋆ **curl** $(V_h^\mu) \subset V_h^\varepsilon$ leads to strong Ampere (in $V_h^\varepsilon$).
  $\longrightarrow$ Can use a larger space $\tilde{V}_h^\varepsilon = (\mathcal{P}_{p-1}(\mathcal{T}_h))^2$ to compute $\mathbf{E}_h$.
- ⋆ Strong Gauss law : $\mathrm{div}(\mathbf{E}_h) = \frac{1}{\varepsilon_0} P_h \rho_h$.

# Galerkin Solver – The conforming / non-confirming scheme

Find $(E_h, \tilde{B}_h) \in \mathcal{C}^1([0,T]; V_h^\varepsilon \times \tilde{V}_h^\mu)$, where $\tilde{V}_h^\mu = \mathcal{P}_p(\mathcal{T}_h)$, solution to

$$\begin{cases} \langle \partial_t E_h, \varphi^\varepsilon \rangle - c^2 \langle \mathbf{curl}\, P_h^\mu \tilde{B}_h, \varphi^\varepsilon \rangle = -\frac{1}{\varepsilon_0} \langle \pi_h^{\mathrm{div}} J, \varphi^\varepsilon \rangle, \quad \varphi^\varepsilon \in V_h^\varepsilon \subset H(\mathrm{div}\,;\Omega) \\ \langle \partial_t \tilde{B}_h, \tilde{\varphi}^\mu \rangle + \langle E_h, \mathbf{curl}\, P_h^\mu \tilde{\varphi}^\mu \rangle + c \langle B_h, \tilde{\varphi}^\mu \rangle_{\Gamma_A} = 0, \quad \tilde{\varphi}^\mu \in \tilde{V}_h^\mu \not\subset H(\mathbf{curl};\Omega) \end{cases}$$

where

- $\pi_h^{\mathrm{div}}$ is the Raviart-Thomas finite element interpolation,
- $P_h^\mu \ : \ \tilde{V}_h^\mu \to V_h^\mu$ is a projection on $V_h^\mu$.

⟶ Strong Ampere equation.

⟶ Strong Gauss law.

⟶ As DG, does not require to invert a global mass matrix.

# The Vlasov Solver

# PIC for Vlasov

The distribution function is approach by $N_p$ macro-particles with positions $x_k^\varepsilon$, velocities $v_k^\varepsilon$ and weights $\omega_k$ :

$$f_{N_p}(x, v, t) = \sum_{k=1}^{N_p} \omega_k \delta(x - x_k(t)) \delta(v - v_k(t)).$$

The macro-particles are advanced along the characteristics :

$$\begin{cases} \dfrac{dx_k}{dt} = v_k, \\ \dfrac{dv_k}{dt} = \dfrac{q}{m}(E(x_k, t) + v^\perp B(x_k, t)), \\ x_k(0) = x_{k,0}, \quad v_k(0) = v_{k,0}, \end{cases}$$

where $(x_{k,0}, v_{k,0})$ realisation of $f_0$.

# Coupling between Maxwell and Vlasov

- Fully discrete Maxwell solver (obtained with **Leap-frog**) takes in **entries** the degrees of freedom of the fields at time $t_n$ and the degrees of freedom of $\pi_h^{\mathrm{div}} J$ at time $t_{n+\frac{1}{2}}$.

⟶ We need to compute a numerical approximation of the degrees of freedom of $\pi_h^{\mathrm{div}} J$ at time $t_{n+\frac{1}{2}}$.

⟶ Computed from the Particles' trajectories on $[t_n, t_{n+1}]$. Known since they are piecewise affine and they only depends on $\mathbf{E}$ and $B$ at time $t_n$ (Leap-frog scheme) :

$$\begin{cases} x_k(t) = x_k^n + v_k^{n+\frac{1}{2}}(t - t_n), \\ v_k(t) = v_k^{n+\frac{1}{2}} = v_k^{n-\frac{1}{2}} + \dfrac{q\Delta t}{m}\left( E_k^n + \dfrac{\left(v_k^{n-\frac{1}{2}} + v_k^{n+\frac{1}{2}}\right)^{\perp}}{2} B_k^n \right), \end{cases}$$

# Coupling between Maxwell and Vlasov

- From early works of Eastwood : charge conserving currents can be obtained by

$$\mathbf{J}^{n+\frac{1}{2}} := q\sum_{k=0}^{N_p} w_k \int_{t_n}^{t_{n+1}} \mathbf{v}_k^{n+1/2} S\left(x - x_k\left(t\right)\right) \frac{\mathrm{d}t}{\Delta t}.$$

- Degrees of freedom of $\pi_h^{\mathrm{div}}(\mathbf{J}^{n+\frac{1}{2}})$ are integrals on the triangle $T$ and on the edge $\mathbf{e}$ of the mesh.

⟶ We will use quadrature formulas

⟶ $\mathbf{x}_{T,j}^{\mathrm{NI}}$ the quadrature points, we have to compute :

$$C_{T,j}^{\mathrm{NI}}(\kappa, n) := \int_{t_n}^{t_{n+1}} S(\mathbf{x}_{T,j}^{\mathrm{NI}} - \mathbf{x}_\kappa(t)) \frac{\mathrm{d}t}{\Delta t}.$$

⟶ Implementation (during the CEMRACS) of a routine with Jacobs & Hesthaven splines.

# Numerical results

# Goals

On two test cases, Diode and Magnetron, we :

- compare FEM-PIC solver and Conga-PIC solver with a strong Ampere scheme,
- compare the calculation of current :

$$\mathbf{J}^{n+\frac{1}{2}} := q \sum_{k=0}^{N_p} w_k \int_{t_n}^{t_{n+1}} \mathbf{v}_k^{n+1/2} S\left(x - x_k\left(t\right)\right) \frac{\mathrm{d}t}{\Delta t},$$

with

$$S = \begin{cases} \delta, \\ \text{B-Spline}, \\ \text{Jacobs and Hesthaven Spline.} \end{cases}$$

$\longrightarrow$ Splines are more regular. Less noise ?

$\longrightarrow$ Jacobs & Hesthaven Splines are simpler. Faster ?

# $\mathbf{J}^{n+\frac{1}{2}}$ : Dirac

- FEM - PIC

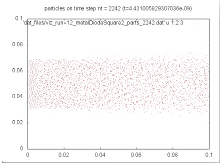


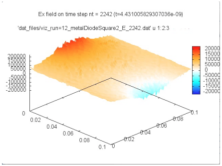


- Conga - PIC

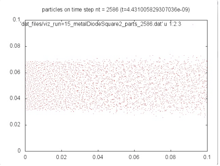


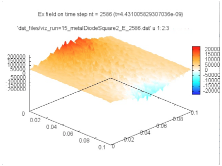


**Conclusion :** Same behavior between FEM-PIC and Conga-PIC.

# $\mathbf{J}^{n+\frac{1}{2}}$ : Jacobs & Hesthaven Spline vs B-Spline

Conga - PIC with Jacobs & Hesthaven Spline

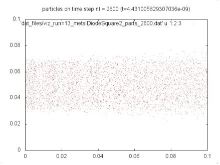


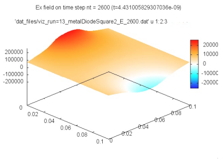


| | Jacobs & Hesthaven Spline | B-Spline |
|---|---|---|
| CPU time | $2052s$ | $2623s$ |

**Conclusion :**

$\longrightarrow$ less noise with Spline than with Dirac

$\longrightarrow$ reduction of CPU time with Jacobs & Hesthaven Spline

# $\mathbf{J}^{n+\frac{1}{2}}$ : Dirac vs Jacobs & Hesthaven Spline

Conga - PIC with Dirac vs Jacobs & Hesthaven Spline

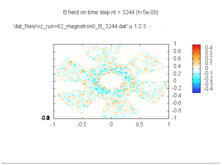


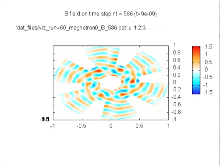

# Conclusion & Perspectives

Conclusion :

- we have adapted the analysis of the Conforming and Conga schemes (with strong Ampere) for the 2D TE Maxwell,
- we have implemented $\pi_h^{\mathrm{div}}(\mathbf{J}^{n+\frac{1}{2}})$ with Jacobs & Hesthaven Splines,
- we have begun numerical comparisons : conforming scheme vs Conga scheme,
- we have compared different kinds of particles : Dirac, Jacobs & Hesthaven Splines and B-Splines,
- we have compared two schemes on several test cases.

Perspectives :

- we have to improve the analysis of the Conforming and Conga schemes for mixed boundary conditions,
- we have to pursue the numerical comparisons : Conforming and Conga with strong Faraday, and DG
- we have to improve the injection (more physical) for the Magnetron test case

# Bibliography

J.-C. Nédélec
Mixed finite elements in $\mathbb{R}^3$ (Num. Math. '80)

P. Monk
An analysis of Nédélec's method for the spatial discretization of Maxwell's equations (JCAM '93)

C.-D. Munz, P. Omnes, R. Schneider, E. Sonnendrücker and U. Voß,
Divergence Correction Techniques for Maxwell Solvers Based on a Hyperbolic Model (JCP '00)

M. Costabel and M. Dauge
Computation of resonance frequencies for Maxwell equations in non-smooth domains (Tcwp '03)

G.B. Jacobs and J.S. Hesthaven
High-order nodal discontinuous Galerkin particle-in-cell method on unstructured grids (JCP '06)

M.L. Stowell and D.A. White
Discretizing transient current densities in the Maxwell equations (ICAP '09)

A. Stock, J. Neudorfer, R. Schneider, C. Altmann and C.-D. Munz
Investigation of the Purely Hyperbolic Maxwell System for Divergence Cleaning in Discontinuous Galerkin based Particle-In-Cell Methods (Coupled Problems '11)

M. Campos Pinto and E. Sonnendrücker
Gauss-compatible Galerkin schemes for time-dependent Maxwell equations (submitted, '14)